JOURNAL OF AIRCRAFT
Vol. 42, No. 2, March–April 2005

Time-Domain Training Signals Comparison for Computational Fluid Dynamics Based Aerodynamic Identification

Charles R. O'Neill* and Andrew S. Arena Jr.†
Oklahoma State University, Stillwater, Oklahoma 74078

Three classes of input training signals are evaluated for computational fluid dynamics based aeroelastic prediction performance. Binary signals, frequency sweeps, and multisines are reviewed and evaluated for aeroelastic prediction performance. Aerodynamic requirements are developed for input signal design and implementation. The input training signals are evaluated with signal property analysis and aeroelastic stability predictions. Five specific input signals were tested with the AGARD 445.6 aeroelastic testcase at Mach 0.90. The signals are the binary 3211 multistep, the frequency swept chirp, the frequency swept offset dc-chirp, the frequency swept Fresnel chirp and the multisine Schroeder sweep. The offset dc-chirp gave the best performance.

Introduction

COMPUTATIONAL finite element analysis of coupled aerodynamic and structural systems provides powerful aeroelasticity analysis and design tools. Finite element methods offer solutions to arbitrary physical configurations at the expense of computational requirements. The STARS analysis program developed by Gupta[1] couples structural and aerodynamic finite element solutions to provide aeroelastic predictions for flight-test support.

The traditional computational fluid dynamics (CFD) based approach to determine stability for a specific configuration requires multiple free response calculations at varied flight conditions. A typical aeroelastic analysis spends 95% of the computational time for the fluid dynamics calculation. The remainder is spent computing the structural response. Replacement of the slow CFD solver with an aerodynamic system model allows for improved efficiency and additional physical insights.[2] The challenge is finding a good system model.

This paper seeks to improve system model quality with improved input training signals. For the aerodynamic system identification routine to capture a useful model, the dominant aerodynamics must be excited. Aerodynamic system identification contains unique requirements not typically seen in traditional system identification. This paper reviews and evaluates basic input signal forms and examines their performance for aerodynamic system identification in the time domain. The goal is to select a robust and implementable input training signal.

Signal Review

The literature provides abundant information on signal design and system identification techniques. Few, if any, signals are designed specifically for CFD applications. Yet, the challenges and requirements facing CFD based identification are unique. The application of well known excitation signals for traditional experimental identifications provides initial criteria and intuition for signal design and selection. The switch from the physical realm to the computational idealization adds additional criteria and requirements.

Received 11 November 2003; presented as Paper 2004-0209 at the 42nd Aerospace Sciences Meeting and Exhibit, Reno, NV, 5–8 January 2004; revision received 19 February 2004; accepted for publication 20 February 2004.

*Graduate Research Assistant, Mechanical and Aerospace Engineering. Student Member AIAA.

†Associate Professor, Mechanical and Aerospace Engineering. Senior Member AIAA.

Input signals designed and evaluated for frequency domain identification are common. Whereas the fundamental requirements for the time domain are similar, identification in the time domain has some subtle differences. Any input signal can be used for time-domain identification[3]; however, the quality of the resulting model will reflect the input signal quality. Although basic system predictions may be possible with simple system models and arbitrary input signals, high-resolution predictions and control system analysis needs high-quality system models.

Certain input signal requirements are fundamental. The input signal must be realizable and implementable. The input signal must excite the system dynamics needed for modeling. The input signal must avoid overdriving the system.[4]

Three signal types are evaluated in this paper: binary signals, frequency sweeps, and multisines. Historically, these signals are commonly used for system identification. For flight testing, binary signals and multisines are common.[5] Other disciplines commonly use the frequency sweep.

Binary Signals

Binary signals consist of a series of pulses arranged for a specified frequency spectrum. The binary signal frequency spectrum unfortunately contains unexcited spectral areas that are filled only by adding significant length to the signal.[6]

Random noise signals are a type of binary signals with variable pulse amplitude. Random noise signals produce a conceptually flat power spectral density (PSD) for infinite excitation lengths. A flat PSD implies equal power at high frequencies, perhaps overdriving the system. Stochastic system theory offers powerful results, especially for linear systems. Yet, Schoukens et al. found that random noise does not automatically average out system nonlinearities.[6]

Binary signals also can be nonrandom. A binary signal, the 3211 multistep, is a commonly used flight-test signal.[3] This may be, in part, because the multistep's functional form is easy to implement. Interestingly, binary signals are not exactly realizable because of excitation system dynamics. Physical binary signal excitations are filtered by nature; purely computational binary signals have no natural filter.

Frequency Sweeps

Frequency sweeps are generated by smoothly varying frequency for a sinusoidal function. By design, all frequencies within a specified bandwidth are excited. Variation of amplitude as a function of frequency almost allows for exact specification of the sweep's PSD. One disadvantage of a sweep is poor low-frequency performance.[7,8] Investigations into improving chirp frequency response are not common; most investigators switch to multisine signals to improve low-frequency response. Numerical difficulties[9] associated with advanced frequency sweep forms are partially responsible for their limited development. Linear frequency sweeps are often called chirps.

Frequency sweeps are common in the flight-test community.[3] One dangerous disadvantage of the frequency sweep is overexcitation of the structure, which often causes critical flight incidences.[3] Even sweeping near a structural or aeroelastic resonance frequency can unintentionally overexcite the structure. A practical disadvantage is that the time to complete a frequency sweep may exceed the time available at a particular flight condition.[10]

Multisine Signals

Multisine signals are generated by the superposition of phased harmonic signals. Exact specification of the PSD form consists of variation of the amplitude for each harmonic. Excitation frequency bands are exactly specifiable by addition of the appropriate frequency set. Gaps in the excitation frequencies bands are allowed. For a discrete time signal, harmonic signals are specified at each measurable frequency.

The classic multisine signal is the Schroeder sweep.[11] Phased discrete frequencies are added to form an arbitrary PSD across a specified bandwidth. The Schroeder sweep visually resembles a frequency sweep.[12] Algorithms for minimization of the multisine peak factor are common.[4,12–14] Simon and Schoukens found that the Schroeder sweep is sensitive to the signal excitation length.[15] Phased multisines have startup problems because of nonzero initial conditions.

Multisines are common in recent flight-test excitation signals.[8,10,16] For a specific helicopter identification problem, Young and Patton found that multisines gave slightly better results than the corresponding frequency sweeps.[7] They attribute this improvement to the multisine's improved low-frequency excitation.

Methodology

The fundamental objective of system identification for this paper is to generate a useful aerodynamic system model for aeroservoelastic predictions. This paper focuses on the development of input training signals to improve the resulting model quality, not the details of how models are created. Aeroservoelasticity is the combination of structural elasticity, aerodynamics, and servocontrols. Reformation of the problem as a coupled structural, aerodynamic, and control system allows for computer simulations.[1] The CFD solver generates flow properties based on structural boundary conditions. The structural solver generates boundary conditions based on flow properties. Solutions in time are generated by time marching forward from a specified initial condition. Practical stability, control, and design analysis is possible when the aerodynamic and structural states of an aeroservoelastic system[2] are coupled.

For system identification, an aerodynamics system model replaces the CFD solver. Ideally, this aerodynamics model will exactly reproduce the aerodynamic outputs with the same boundary condition inputs. Aerodynamic system identification requires development of a model based on input and output relationships. The process is shown conceptually in Fig. 1. The process inputs a known motion into the aerodynamic system. The CFD solver uses this input motion to calculate unsteady aerodynamic forces. The objective of system identification is to determine a system that fits the training data. The relationship between the generalized motions and forces is used to synthesize the parameters of the system model. Once the system model is determined, the generalized forces resulting from arbitrary generalized motion inputs can be found.

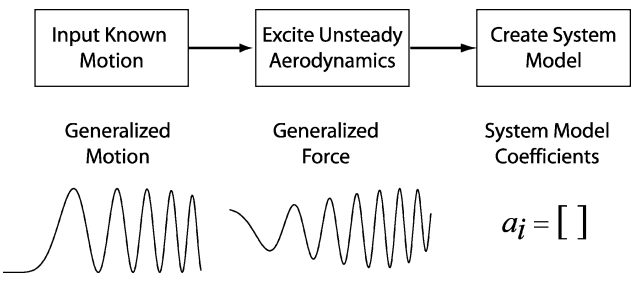

Fig. 1 System identification process.

Determination of model parameters is a demanding problem because possible solution sets are not unique.[17] Whereas any input–output data set can be used to develop a system model, an optimal system model, the implied goal of system identification, requires a carefully crafted input signal. The system model may exactly reproduce the training signal, but not contain the relevant physics. Quality training signal characteristics are critical for determination of useful models.

Input signal design starts with investigation of the physical system. System knowledge will provide useful guidelines on how best to excite, measure, identify, and use the resulting model. For aerodynamics, a generalization of the input vs output relationship is made through theoretical unsteady aerodynamics solutions. For example, the classical Theodorsen, Sears, and sectionally analytic unsteady solutions indicate that output forces are varied in phase and magnitude from the input motion. These classical incompressible unsteady aerodynamics solutions include boundary condition derivatives up to acceleration.

An assumed solution for a general aerodynamics problem is developed for input motions and output forces. The output force depends on both the force dynamics f and the input motion dynamics x. The $f(t-t_f)$ and $x(t-t_x)$ terms account for pure delays. A static offset f_0 is included to permit operation around a nonzero equilibrium condition:

$$\underbrace{f^{(n)} + \cdots + \ddot{f} + \dot{f} + f + f(t-t_f) + f_0}_{\text{internal response}} = \underbrace{x^{(m)} + \cdots + \ddot{x} + \dot{x} + x + x(t-t_x)}_{\text{input response}}$$

This continuous time model directly extends to a discrete time model for CFD based training data. The problem is now reduced to a typical system identification problem.

Excitation Requirements

The input signal excitation must satisfy specific requirements based on physics and system theory. Additionally, unsteady CFD based aerodynamics impose additional requirements. The input signal is coupled to the CFD solver only through motion boundary conditions. Both CFD boundary conditions, displacement and velocity, are required. The following requirements are imposed: 1) excitation of both input motion and output force dynamics for displacement based linear identification, 2) steady-state aerodynamic starting condition, and 3) consistent displacement and velocity discrete-time motion boundary conditions.

The first criterion is that the input signal must excite the system in a way that is consistent for linear aerodynamics system identification. The signal must allow the static offset forces to be determined. Additionally, the signal magnitudes must be large enough to excite the dominant unsteady aerodynamics while still being kept in the linear aerodynamics range. The objective function shows that both input and output dynamics must be excited. Comparison with the Theodorsen unsteady aerodynamic theory indicates that the excitation must excite both noncirculatory and circulatory lift in a way that allows the system model to distinguish between the two.

Spectral power requirements set another input signal criterion. The input signal must excite the aerodynamic system with sufficient power over a useful frequency range. A smooth PSD across a specifiable frequency band is preferred. The input boundary conditions are coupled, and so flat PSDs are not possible for both displacement and velocity. Integration transforms a hypothetically flat PSD signal to a decreasing PSD with slope −20 dB per decade. Specification of a flat PSD for displacement yields an input signal with a poor low-frequency velocity PSD. Coupled boundary conditions create PSD design and selection difficulties.

An undesirable situation occurs when unknown nonlinearities are incorrectly attributed to linear model parameters. The system model is linear, and so avoidance of large input and output magnitudes is beneficial. The ratio of maximum value to average value, peak factor, becomes a useful criterion. Input signal peak factor minimization is

necessary.[11] Broad PSDs are desired, but so are small peak factors. PSD and peak factor are often direct tradeoffs.

A physics based steady-state starting condition restriction is imparted on the excitation signal. The training data must have an initial steady-state flow solution and start from zero motion to ensure unsteady flow solution accuracy and to allow the model to associate the outputs with valid inputs. This condition significantly restricts the choice of input signals presented in the literature. Specifically, this restricts input signals to motions with step changes, zero frequency starting conditions, or envelopes.

An additional criterion is placed on the excitation signal because the model representation form only uses modal displacements for input correlation. The excitation must train all input motion parameters based on displacement; however, both displacement and velocity are required for CFD motion specification. Because the goal of the aerodynamic system model is to match the CFD solution, this boundary condition criterion implies that the training signal needs to use the same motion update characteristics as the coupled aeroelastic system.

Performance Evaluation

The final determination of an input signal's suitability is its performance. It is not enough that the input signal generates reproducible data from the system model; the input signal must produce useful and physically consistent data. Coupling the aerodynamic model with structural and controls models often introduces unexpected behavior. Any input signal selection criteria must include couple system prediction performance.

The stability boundary is computed as the dynamic pressure necessary to push an eigenvalue outside the discrete time unit circle in the z plane. This paper will evaluate signal performance with two aeroelastic stability boundary criteria.

First, the system model stability boundary prediction must match the traditional CFD boundary prediction. Matching the traditional CFD boundary ensures a useful aerodynamic system model.

Second, a monotonic stability boundary convergence with increasing system model order is desired. Faster convergence indicates more robust system training.

Training Signals

This section concerns input signal design. Three fundamental signal classes are presented: binary signals, frequency sweeps, and multisines. Six specific signals are presented: the 3211 multistep and noise in the binary class; the chirp, dc-chirp, and Fresnel in the frequency sweep class; and the Schroeder sweep in the multisine class.

Multistep

The 3211 multistep signal consists of a unit step of lengths 3, 2, 1, and 1 unit implemented on velocity. Figure 2a shows the displacement and velocity for the multistep. Displacement is determined with numerical velocity integration. A displacement dc offset occurs because the velocity signal is not symmetrical.

A multistep's displacement and velocity PSD is given in Fig. 2b. PSD magnitude is plotted on a log scale; frequency is plotted as a nondimensional ratio of Nyquist frequency. Changing the multistep's length does not affect the PSD form, but does change the total power magnitudes. The displacement PSD displays the characteristic -20 dB per decade decrease in power when compared to the velocity PSD. The multistep has the following advantages. The stepped velocity boundary conditions make the 3211 multistep easy to implement. The starting-from-rest condition is automatically satisfied. Additionally, the maximum motion magnitudes are known in closed form. The excitation frequency spectrum covers a wide range with good low-frequency content.

There are several disadvantages to the multistep signal. First, the multistep does not excite the higher-order terms in a consistent manner because the multistep has step inputs in velocity. Acceleration training data are limited to one time step after each change in velocity. Any unsteady forces due to acceleration terms will be captured in a non-physical manner. The second problem with the multistep is

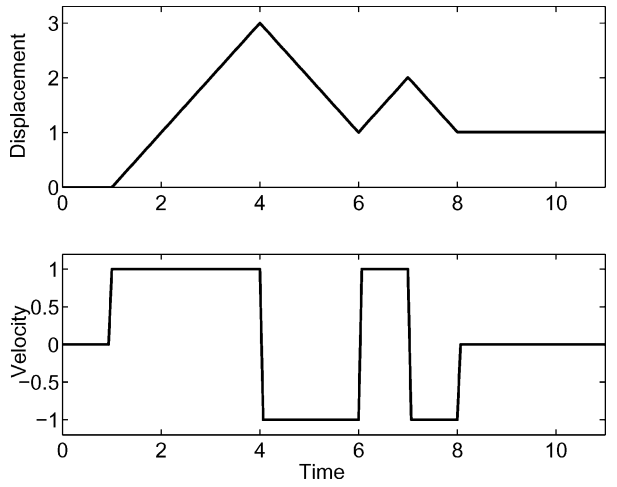

a) Multistep motion form

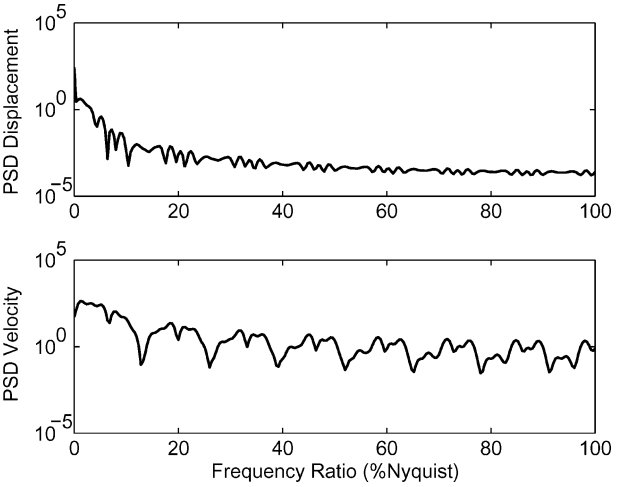

b) Multistep PSD

Fig. 2 Multistep motion and PSD.

that the PSD contains spectral holes. Particular frequencies are not excited. Input signals with excitation holes create system models with poor transfer function properties. A third disadvantage occurs because the velocity is strictly specified. Nonsimultaneous motion state vector updates cause inconsistencies in motion boundary conditions. A final disadvantage to the multistep is that the length sizing of the multistep is not intuitive.

Chirp

The chirp input signal belongs to the frequency sweep class of input signals. These signals allow for smooth transitions in a specific frequency range. The chirp is a linear frequency sweep and analytic everywhere. The chirp form is

$$d(t) = \sin \omega t^2, \qquad v(t) = 2\omega t \cos \omega t^2$$

A time history plot of the chirp's motion for displacement, velocity, and acceleration is given in Fig. 3a. The displacement is centered around zero with an amplitude of one. The velocity envelope increases linearly with time.

The chirp's displacement has a constant amplitude, so that the PSD in Fig. 3b is conceptually flat for displacement and is sloped at $+20$ dB per decade for velocity.

The chirp has the following advantages. First, the chirp is an analytic function. The chirp is consistent with the system model function and is capable of exciting all aerodynamic motion terms. The chirp starts from zero frequency and zero motion at time zero. The chirp's displacement PSD is conceptually flat up to the maximum excitation sweep frequency. The chirp also has an intuitive and easily determined frequency excitation description.

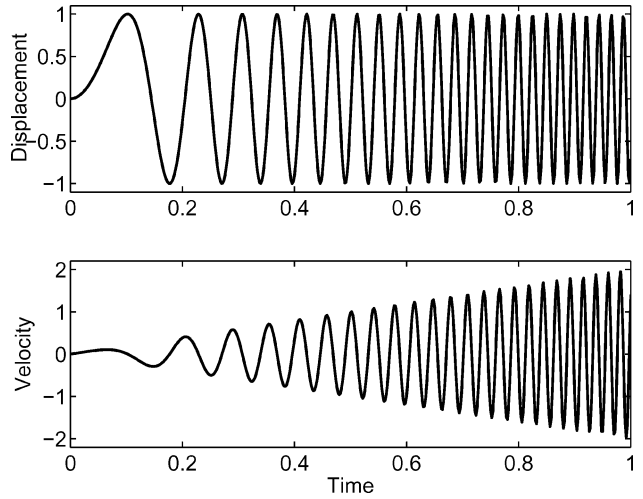

a) Chirp motion form

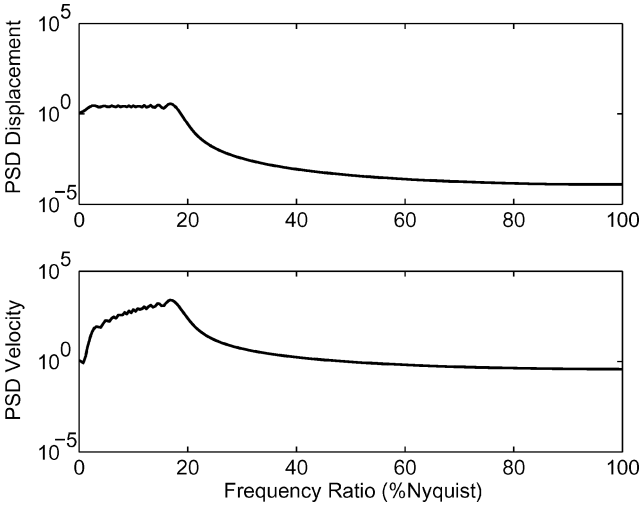

b) Chirp PSD

Fig. 3 Chirp motion and PSD.

Two major disadvantages occur for the chirp. First, the low-frequency performance of the chirp is poor for displacement and even worse for velocity. The chirp's velocity PSD contains a poorly excited low-frequency region, exactly where most aerodynamic predictions are concentrated. Improved low-frequency excitation, without sacrificing the higher-frequency excitation, will require either a nonlinear frequency sweep or a long excitation. From the Theodorsen function, the largest phase difference for unsteady aerodynamics occurs at low reduced frequencies. The second disadvantage results from the analytic nature of the chirp. Because the chirp is analytic, the system model only contains analytic motion information. Nonanalytic motions may not be accurately represented by the resulting aerodynamic system model.

DC-Chirp

The dc-chirp contains a static offset to alleviate the low-frequency problems inherent in the basic chirp signal. The result is an asymmetrical signal with a similar form but with improved low-frequency performance when compared to the chirp excitation signal. The functional form is

$$d(t) = (1 - \cos \omega t^2)/2, \qquad v(t) = \omega t \sin \omega t^2$$

The dc-chirp's form is based on the original chirp but with a nonzero static offset. The offset increases the low-frequency power. The signal is a linear frequency sweep from zero frequency at time zero. Like the original chirp, the signal is analytic everywhere.

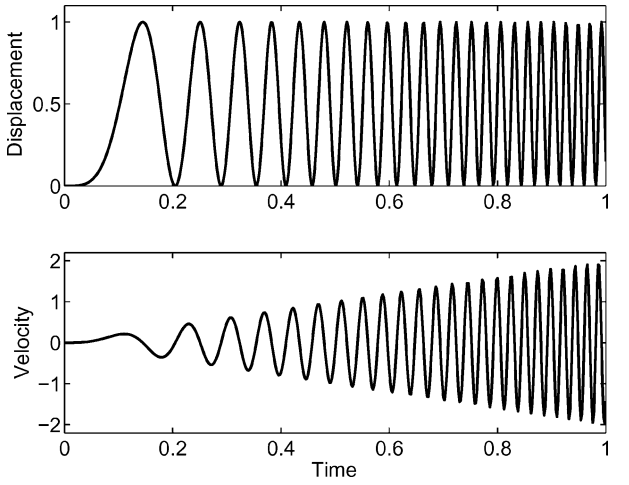

a) DC-chirp motion form

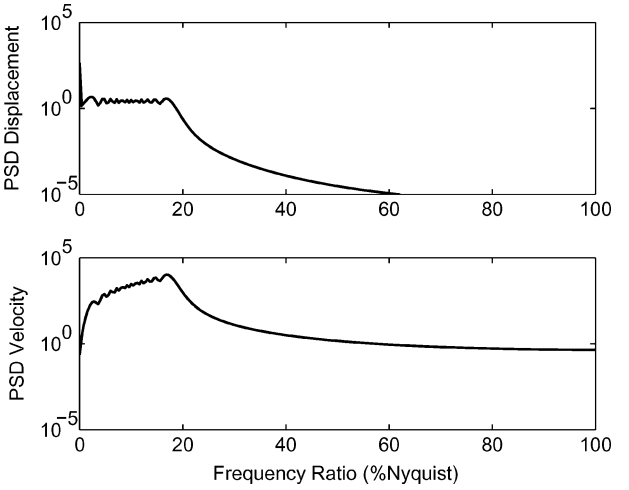

b) DC-chirp PSD

Fig. 4 DC-chirp motion and PSD.

The dc-chirp's PSD is given in Fig. 4b. The PSD form remains similar to the chirp's form. The dc offset increases the displacement power at near-dc low frequencies. Low-frequency velocity power is not substantially improved, as expected, when compared to the original chirp's PSD.

The dc-chirp has the same advantages as the original chirp, plus additional low-frequency displacement power. The dc offset adds the low-frequency power. The dc-chirp allows for a visual determination of rate and displacement effects because the displacement motion is offset and the velocity is symmetrical. The asymmetrical motion forms allow for improved distinction between the effects of displacement and velocity.

The dc-chirp has similar disadvantages as the original chirp. Addition of the dc offset removed the PSD problem at low frequencies for the displacement; however, the low-frequency velocity PSD is still poor. A subtle second disadvantage concerns the peak factor of the dc-chirp compared to the original chirp. Because the new dc-chirp is asymmetrical, the absolute forced magnitude of displacement is only one-half that of the original chirp for a given maximum displacement. Doubling the dc-chirp's magnitude to achieve a similar power level pushes the aerodynamics closer to undesired nonlinear regimes.

Fresnel Chirp

The Fresnel chirp is a linear frequency sweep with a displacement as the integral of the original chirp. The Fresnel chirp is expected to increase the low-frequency velocity power. The result is an excitation signal with no closed-form expression but with potential for better training performance.

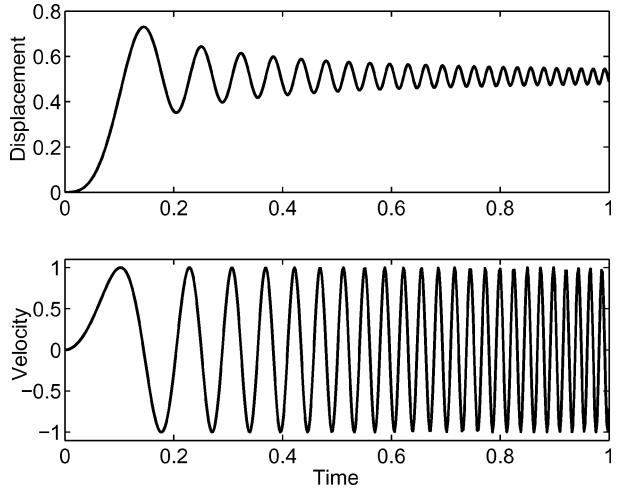

a) Fresnel motion form

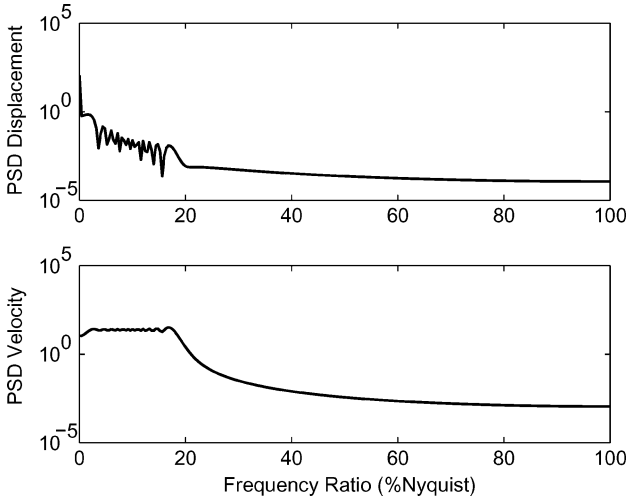

b) Fresnel PSD

Fig. 5 Fresnel chirp motion and PSD.

The Fresnel chirp is an integrated form of the original chirp. The Fresnel chirp, shown in Fig. 5a, contains a linear frequency sweep and is analytic everywhere. As a practical implementation issue, there are two forms of the Fresnel chirp. The two forms result from the integration of either the sine or cosine function. The signal needs to start from rest, and so the Fresnel sine function $S(t)$ is chosen. The functional form is

$$d(t) = \int_0^t \sin \omega\tau^2 \, d\tau = S(t), \qquad v(t) = \sin(\omega t^2)$$

The Fresnel chirp has conceptual improvements over the chirp and dc-chirp frequency-sweep signals. The largest improvement is the flat velocity PSD. Like the chirp, the Fresnel's velocity PSD decays at near-zero frequencies.

Unlike the progression from the chirp to the dc-chirp, an integrated Fresnel chirp cannot be implemented because integration of an asymmetrical signal produces a diverging signal, which eventually violates linearity restrictions for large excitation bandwidths.

Another disadvantage of the Fresnel chirp is that the resulting function has no simple, closed-form solution and requires numerical integration for practical implementation.[9] The integration scheme appears to be introducing noise into the displacement signal, which results in a noisy displacement PSD. Noisy integration may become a sensitivity issue later.

Schroeder Multisine

The Schroeder excitation signal is multisine class signal. A summation of discrete frequencies allows for the specific excitation of an exactly specified bandwidth. A phase shift presented by Schroeder[11] minimizes the signal's peak factor.

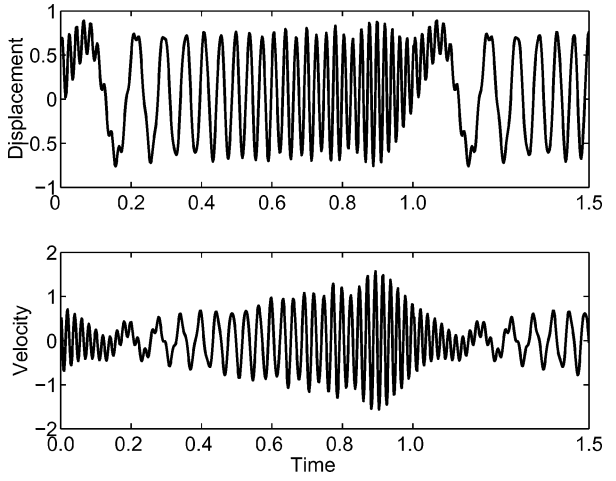

a) Schroeder motion form

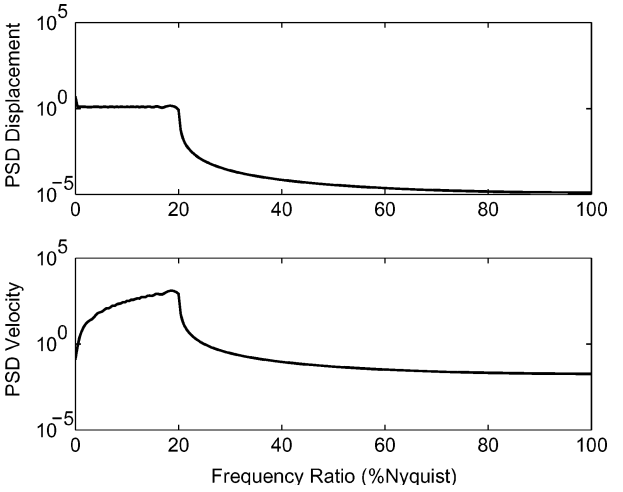

b) Schroeder PSD

Fig. 6 Schroeder multisine motion and PSD.

The Schroeder form is based on a sum of cosine terms with a specified phasing. Expressions for displacement and velocity are given hereafter. The form is analytic in time and is discrete in frequency:

$$d(t) = \sum_{k=1}^{N} \sqrt{\frac{1}{2N}} \cos\left(\frac{2\pi kt}{T} - \frac{\pi k^2}{N}\right)$$

$$v(t) = \sum_{k=1}^{N} \frac{-2\pi k}{T} \sqrt{\frac{1}{2N}} \sin\left(\frac{2\pi kt}{T} - \frac{\pi k^2}{N}\right)$$

The signal, shown in Fig. 6a, is harmonic and can continue indefinitely. The signal resembles a frequency sweep during a significant portion of the time history. The Schroeder sweep appears to be the discrete-time counterpart to the continuous-time frequency-swept chirps.

A PSD for the Schroeder sweep is given in Fig. 6b. The number of terms in the summation determines the sweep bandwidth. The PSD is flat along the specified excitation bandwidth. This particular signal excites up to 20% of the Nyquist frequency. The sweep is implemented on displacement, so that the velocity PSD exhibits the expected sloped response.

The Schroeder sweep has the following advantages. First, the PSD is specified in an intuitive manner and is flat. The Schroeder sweep at zero frequency has desirable power levels for the excitation motion. Second, the Schroeder sweep has an optimal peak factor when compared with both discrete and continuous sweep signals.

The disadvantages are concentrated in three areas. First, the Schroeder sweep does not intrinsically contain a from-rest starting condition. Any attempt to use the Schroeder sweep requires a change to establish both the steady-state system behavior and the from-rest starting response. If the sweep is bound with an envelope, this will cause undesirable and nonintuitive distortions of the signal's characteristics. Simon and Schoukens[15] show the undesirable results of harmonic signal truncation. Second, the Schroeder sweep requires a numerical sum of terms at each time step. This summation is expensive for large excitation bandwidths. The third disadvantage is that the Schroeder sweep appears excessively sensitive to excitation length. Testing shows that small errors in signal specification can cause regular holes in the Schroeder's PSD. These types of sensitivities are not desired for robust training.

Random Noise

A final class of signals is based on stochastic system theory. White noise is defined as a signal with equal power at all frequencies. A white noise input signal allows for equal excitation up to the Nyquist frequency. Excitation length strongly determines the PSD distribution characteristics. A constant PSD over the entire frequency range requires an infinite excitation length.

The white noise input signal has advantages. First, the PSD is defined to be flat. The signal can start from rest and has no restrictions on excitation length. Unlike the analytic signals, the white noise input will excite the nonharmonic components in the aerodynamic system.

There are numerous disadvantages to the white noise signal. First, the flat power level is only achievable as the excitation length becomes infinite. The excitation length requirement is not intuitive. The fundamental implementation question becomes, how long is long enough? A related disadvantage is that the training signal is not deterministic. The noise input signal is not guaranteed to excite the same system dynamics between two otherwise identical simulations.

Second, the noise input signal creates problems with boundary conditions in two ways. The first is that the input excitation is not consistent with the discrete-time solution method. Equal power at the high frequencies forces large motion derivatives. These changes will overdrive the flow solution solver and violate the linearity assumption. Second, simultaneous updating of motion states is not possible. Because the signal is not deterministic, generation of displacement from velocity, or vice versa, requires numerical integration. Numerical integration introduces time lags and is not consistent with the system model motion specification. These disadvantages suggest a rejection of the noise input signal for CFD based aeroelastic training.

Flutter Prediction Comparisons

Evaluation of the input signal's performance is performed by determination of the aeroelastic response of the system model. Multiple aerodynamic system models are generated for ranges of both motion and internal model orders. The generation process follows Fig. 1. The comparison method is to generate flutter stability boundary predictions and to compare the resulting flutter boundary for varied model orders and input signal types. Sensitivity plots are generated by comparison of the instability boundary dynamic pressure with the model order. A perfect aerodynamic system model monotonically converges to a single flutter boundary prediction as the system model increases in complexity.

A review of the Methodology section assists in the comparison process. The system model has two variables: motion model order and internal system model order. The motion model order defines the number of past motion values used to predict current forces. The internal model order defines the number of past forces used to predict the current forces. Capture of a model of the dominant physics requires convergence of both model orders. The convergence rate depends on the excitation quality. The aerodynamic model's prediction quality and convergence characteristics indicate the input excitation signal's quality.

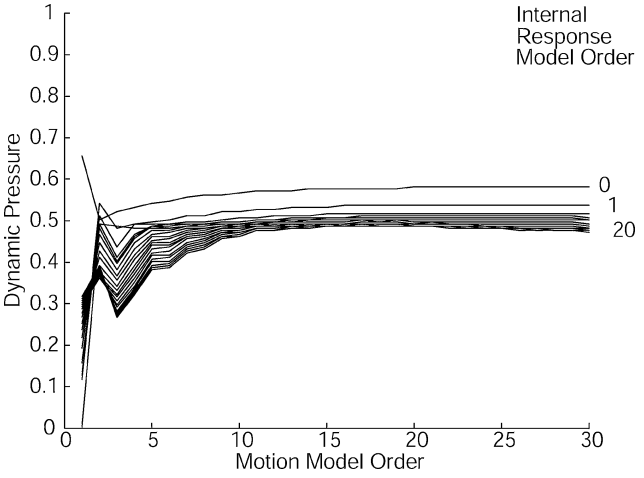

Fig. 7 AGARD 445.6 multistep sensitivity.

This paper presents CFD based results from the AGARD 445.6 aeroelastic test case at Mach 0.90. Euler3d, an unstructured finite element compressible inviscid solver distributed with STARS,[18] is used for all CFD computations. The conclusions based on additional aeroelastic and aeroservoelastic testcases exhibit results and characteristics consistent with this AGARD testcase.[19]

The AGARD 445.6 testcase presents an aeroelastic structure typical of high-performance aircraft. The AGARD 445.6's aeroelastic flutter boundaries at subsonic and transonic Mach numbers were experimentally determined at NASA Langley Research Center in the 1960s (Ref. 20). The AGARD structure consists of a cantilevered wing fixed at the root. The wing has an aspect ratio of 4.0, a quarter-chord sweep of 45 deg and a taper ratio of 0.6. The airfoil is a NACA 65A004. At the tested Mach number, 0.90, transonic flow occurs over the outboard quarter of the wing. The traditional free response CFD simulation predicts a stability dynamic pressure of 0.62 psi.

A training signal investigation was performed for the AGARD at Mach 0.90. The compared signals are the multistep, chirp, dc-chirp, Fresnel chirp, and the Schroeder sweep.

Multistep

The first input signal sensitivity plot is for the 3211 multistep. Figure 7 shows the flutter boundary dynamic pressure and the model orders. The system converges with increasing motion and internal response model orders. As expected from the Training Signal section, the multistep flutter prediction converges slowly to the wrong boundary because the multistep poorly excites the higher-order aerodynamics. Comparison with the other signals also shows that an increase in the internal-response-model-order converges the boundary prediction only slowly, which again indicates poor higher-order aerodynamic training.

Chirp

The chirp sensitivity plot is given in Fig. 8a. The boundary predictions converge for motion model orders greater than five, yet the predictions continually decrease as the model order increases further. A double-bump convergence occurs for the chirp flutter boundary. The first convergence appears at a motion model order of six. The final convergence occurs at a slightly lower dynamic pressure of 0.58 psi. Interestingly, a motion model order of six consistently becomes the first non-scattered prediction for the AGARD flutter boundary with the frequency sweep signals.

DC-Chirp

The dc-chirp sensitivity plot, Fig. 8b, shows improved results. Convergence occurs for motion model orders greater than six. Comparison of the dc-chirp with the original chirp flutter boundaries shows the influence of low-frequency excitation. An increase in the low-frequency power improves the boundary prediction and the

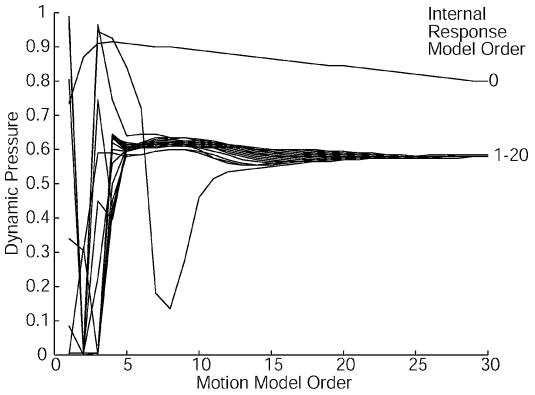

a) Chirp sensitivity

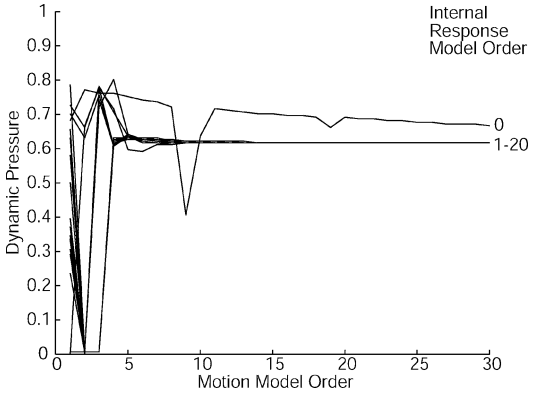

b) DC-chirp sensitivity

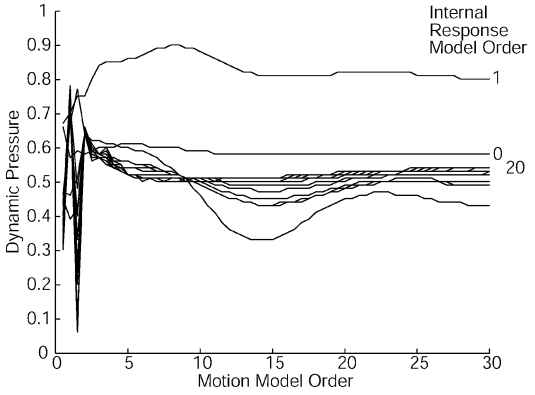

c) Fresnel sensitivity

Fig. 8 AGARD 445.6 frequency sweep sensitivities.

convergence rate. Convergence appears monotonic at a dynamic pressure of 0.62 psi, exactly the traditional CFD free response boundary prediction. The dc-chirp does not exhibit the chirp's double-bump convergence characteristic. A convergence characteristics comparison also suggests that vastly increasing model order compensates for poor excitation, but that the boundary quality remains poor. The multistep also appears to exhibit this convergence vs quality tradeoff. Regardless, the dc-chirp shows excellent prediction quality and convergence properties.

Fresnel Chirp

The Fresnel sensitivity plot, Fig. 8c, shows poor results. The boundary predictions do not monotonically converge, even for model orders of 60. The regular holes in the PSD for displacement appear to cause system model generation difficulties. The sensitivities suggested in the Signal Review section, caused by the Fresnel's lack of a closed-form solution for displacement seem to cause difficulties with the displacement based aerodynamic system model.

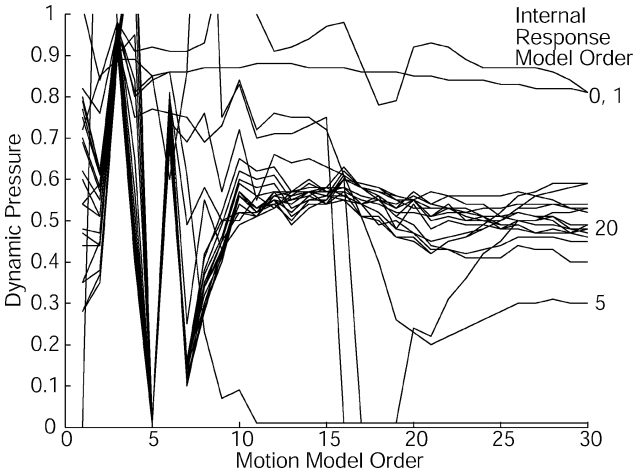

Fig. 9 AGARD 445.6 Schroeder multisine sensitivity.

Schroeder Sweep

The Schroeder sweep sensitivity plot (Fig. 9) shows poor results. To implement the Schroeder sweep, a ramp-up envelope bounded the signal to zero motion at time zero. The stability boundary does not converge quickly and does not converge to the established CFD stability boundary prediction. The Schroeder multisine performs worse than the multistep.

The Schroeder's stability boundary is not consistent. A possible convergence occurs near a motion model order of 10 to 20, but the convergence does not remain for higher model orders. Unlike the frequency sweeps, the Schroeder multisine does not have an initial convergence near a motion model order of 6.

Even though the multisine signals resemble the frequency sweeps, the multisine signals remain harmonic. Power at a specific frequency is distributed across the entire signal. A change of one section of the signal influences the PSD for all frequencies. Implementation of the Schroeder signal requires an envelope on motion, which appears to distort the Schroeder signal's conceptually desirable properties. From the Signal Review section, Schroeder signal sensitivity is expected (see Ref. 15).

Summary

This paper investigated input training signals for CFD based discrete-time aerodynamic system identification. Three signal types are reviewed and evaluated: binary signals, frequency sweeps, and multisines. Training signal criteria were formed to assist with selection and development of new signals. Coupled motion boundary conditions are shown to complicate the selection of a excitation training signal. Unsteady CFD aerodynamic predictions contain unique system identification challenges, especially for boundary conditions and steadystate starting requirements.

The binary signals were reviewed and found to have undesirable traits. Sensitivities appear to limit the usefulness of multisines. Frequency sweeps appear robust and implementable. Displacement based training seems to prefer a flat displacement PSD over a flat velocity PSD. Additional low-frequency power improves coupled aeroelastic prediction accuracy. The dc-chirp gave the best performance for CFD based aerodynamic system identification.

Acknowledgments

Funds for this research effort were provided by NASA Dryden Flight Research Center, NASA Space Grant, and Oklahoma State University.

References

[1]Gupta, K. K., "Development of a Finite Element Aeroelastic Analysis Capability," *Journal of Aircraft*, Vol. 33, No. 5, 1996, pp. 995–1002.

[2]Cowan, T. J., Arena, A. S., and Gupta, K. K., "Accelerating Computational Fluid Dynamics Based on Aeroelastic Predictions Using System Identification," *Journal of Aircraft*, Vol. 38, No. 1, 2001, pp. 81–87.

[3]Miller, D., "A Time-Domain Approach to z-Domain Model Identification," *International Journal of Control*, Vol. 44, No. 5, 1986, pp. 1285–1295.

[4]Braun, M., Ortiz-Mojica, R., and Rivera, D., "Application of Minimum Crest Factor Multisinusoidal Signals for 'Plant Friendly' Identification of Nonlinear Process Systems," *Control Engineering Practice*, Vol. 10, No. 3, 2002, pp. 301–313.

[5]McCormack, A., Godfrey, K., and Flower, J., "Design of Multilevel Multiharmonic Signals for System Identification," *IEEE Proceedings on Control Theory and Applications*, Vol. 142, No. 3, 1995, pp. 247–252.

[6]Schoukens, J., Pintelon, R., Van Der Ouderaa, E., and Renneboog, J., "Survey of Excitation Signals for FFT Based Signal Analyzers," *IEEE Transactions on Instrumentation and Measurement*, Vol. 37, No. 2, 1988, pp. 342–352.

[7]Young, P., and Patton, R., "Comparison of Test Signals for Aircraft Frequency Domain Identification," *Journal of Guidance, Control, and Dynamics*, Vol. 13, No. 3, 1990, pp. 430–438.

[8]Brenner, M., Lind, R., and Voracek, D., "Overview of Recent Flight Flutter Testing Research at NASA Dryden," NASA TM-4792, April 1997.

[9]Zwillinger, D., *CRC Standard Mathematical Tables and Formulae*, CRC Press, Boca Raton, FL 1996, Chap. 6.

[10]Bosworth, J. T., and Burken, J. J., "Tailored Excitation for Multivariable Stability-Margin Measurement Applied to the X-31A Nonlinear Simulation," NASA TM-113085, Aug. 1997.

[11]Schroeder, M., "Synthesis of Low-Peak-Factor Signals and Binary Sequences with Low Autocorrelation," *IEEE Transactions on Information Theory*, Vol. 16, No. 1, Jan. 1970, pp. 85–89.

[12]Van Der Ouderaa, E., Schoukens, J., and Renneboog, J., "Peak Factor Minimization of Input and Output Signals of Linear Systems," *IEEE Transactions of Instrumentation and Measurement*, Vol. 37, No. 2, 1988, pp. 207–297.

[13]Mehra, R., "Optimal Inputs for Linear System Identification," *IEEE Transactions on Automatic Control*, Vol. 19, No. 3, 1974, pp. 192–200.

[14]Mehra, R., "Optimal Inputs for Parameter Estimation in Dynamic Systems—Survey and New Results," *IEEE Transactions on Automatic Control*, Vol. 19, No. 6, 1974, pp. 753–768.

[15]Simon, G., and Schoukens, J., "Robust Broadband Periodic Excitation Design," *IEEE Transactions on Instrumentation and Measurement*, Vol. 49, No. 2, 2000, pp. 270–274.

[16]Brenner, M., "Wavelet Analysis of F/A-18 Aeroelastic and Aeroservoelastic Flight Test Data," NASA TM-4793, April 1997.

[17]Björk, Å., *Numerical Methods for Least Squares Problems*, Society for Industrial and Applied Mathematics, Philadelphia, 1996.

[18]Gupta, K. K., "STARS—An Integrated Multidisciplinary, Finite-Element, Structural, Fluids, Aeroelastic and Aeroservoelastic Analysis Computer Program," NASA TM-4795, April 2001.

[19]O'Neill, C. R., "Improved System Identification for Aeroservoelastic Predictions," M.S. Thesis, Dept. of Mechanical and Aerospace Engineering, Oklahoma State Univ., Stillwater, OK, Aug. 2003.

[20]Yates, E. C., "AGARD Standard Aeroelastic Configurations for Dynamic Response. Candidate Configuration I.—Wing 445.6," NASA TM-100492, Aug. 1987.